

Two-step approaches for effective bridge health monitoring

Jong Jae Lee[†]

*Department of Civil & Environmental Engineering, University of California Irvine,
Irvine, CA, 92697, USA*

Chung Bang Yun[‡]

*Smart Infra-Structure Technology Center, Korea Advanced Institute of Science and Technology,
Yusong-gu, Daejeon 305-701, Korea*

(Received May 17, 2005, Accepted February 3, 2006)

Abstract. Two-step identification approaches for effective bridge health monitoring are proposed to alleviate the issues associated with many unknown parameters faced in real structures and to improve the accuracy in the estimate results. It is suitable for on-line monitoring scheme, since the damage assessment is not always needed to be carried out whereas the alarming for damages is to be continuously monitored. In the first step for screening potentially damaged members, a damage indicator method based on modal strain energy, probabilistic neural networks and the conventional neural networks using grouping technique are utilized and then the conventional neural networks technique is utilized for damage assessment on the screened members in the second step. The effectiveness of the proposed methods is investigated through a field test on the northern-most span of the old Hannam Grand Bridge over the Han River in Seoul, Korea.

Keywords: bridge health monitoring; two-step approach; modal strain energy; probabilistic neural networks; neural networks; field tests.

1. Introduction

Bridge structures are national assets on which socio-economic vitality of the nation depends significantly. They are exposed to various external loads such as traffic, earthquakes, gusts, and wave loads during their lifetime. The structures may get deteriorated and degraded with time in unexpected ways, which may lead to structural failures causing costly repair and/or heavy loss of human lives. Consequently, structural health monitoring has become an important research topic in conjunction with damage assessment and safety evaluation of structures. The use of system identification approaches for damage detection has been expanded in recent years due to the improvement of structural modeling techniques that incorporate response measurements and the

[†] Post-doctoral Researcher, E-mail: jongjael@uci.edu

[‡] Professor, Corresponding author, E-mail: ycb@kaist.ac.kr

advancements in signal analysis and information processing capabilities.

The structural health monitoring (SHM) systems are generally composed of two major parts: (1) hardware, such as sensors, data acquisition equipment, data transmission systems, etc., and (2) software, to perform signal processing, information processing, damage assessment algorithms, information display and management, etc. The first part of SHM systems involves the observation of the structure by means of periodically sampled response measurements from arrays of sensors, storage of the measured data, and transmission of the data to the control center. In the second part involves the extraction of the damage-sensitive features from the measurements, by using various signal/information processing techniques, and the application of damage assessment algorithms to determine the current state of structural integrity. Since the number of bridges equipped with a monitoring system has increased, it has become more necessary to develop an effective damage assessment algorithm based on the measured data.

Usually four levels of damage identification (detection, localization, quantification, and prediction) are discriminated (Rytter 1993) as: (1) Level I methods to identify if damage has occurred (Vandiver 1975, Crohas and Lepert 1982); (2) Level II methods to identify if damage has occurred and simultaneously determine the location of damage (Cawley and Adams 1979, Chance *et al.* 1994); (3) Level III methods to identify if damage has occurred, determine the location of damage, and estimate the severity of the damage (Wu *et al.* 1992, Kim and Stubbs 1995, Yun *et al.* 2001, Lee *et al.* 2002); and (4) Level IV methods to identify if damage has occurred, determine the location of damage, estimate the severity of damage, and evaluate the impact of damage on the structure (Stubbs *et al.* 2000).

Most damage detection methods are based on optimization and parameter identification algorithms comprising one-step scheme by which various levels of damage identification are pursued. When these conventional methods are applied to large-scale redundant structures, ill-conditioning and non-uniqueness in the solution of inverse problems are inevitable difficulties. Moreover, it is not efficient to use Level III and/or Level IV methods in the viewpoint of on-line monitoring. Level I and/or Level II methods should be always incorporated in the monitoring system, whereas Level III and/or Level IV can be applied separated from the monitoring system, only when alarming of damage has occurred.

In this study, the neural networks technique based on the estimated modal parameters is utilized for element-level damage detection. When the neural networks technique is used for damage detection, the number of unknown parameters is related to the network complexity which may cause the ill-conditioning problem. Two-step identification strategies were proposed for effective monitoring of bridge structures to alleviate ill-posedness problem in the neural networks-based damage detection. Two-step approaches for effective bridge health monitoring are briefly addressed. Then the proposed methods are applied in a field test on the Hannam Grand Bridge in Seoul, Korea.

2. Two-step approaches for effective bridge health monitoring

The process of structural health monitoring involves the definition of potential damage scenarios for the system, the observation of the system over a period of time using periodically spaced measurements, the extraction of features from these measurements, and the analysis of these features to determine the current state of health of the system. In this study, the reduction of

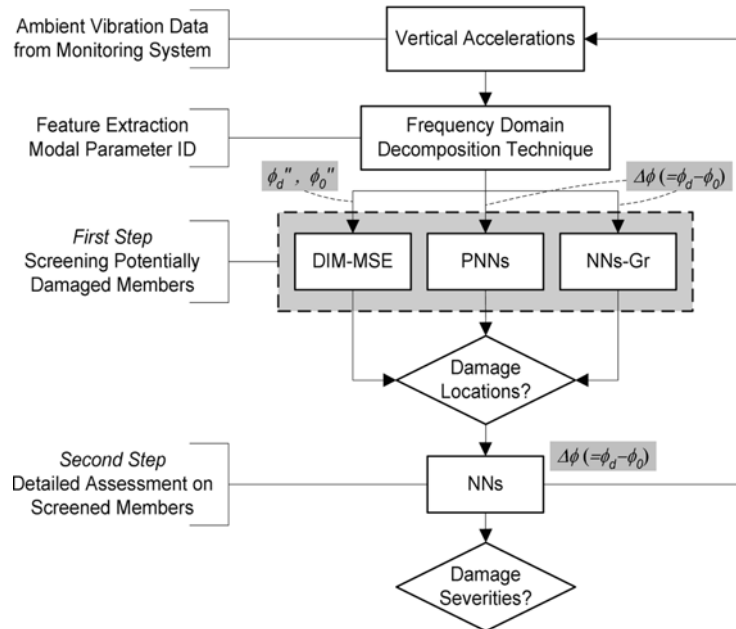
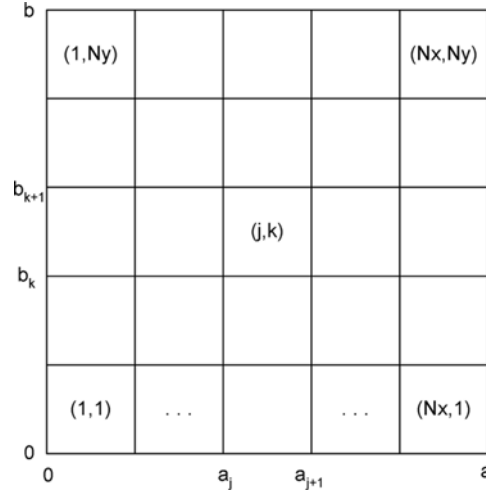


Fig. 1 Flowchart for effective bridge health monitoring

bending stiffness of each element is defined as damage to be estimated. The acceleration data are utilized to identify the modal parameters of a test bridge using the frequency domain decomposition technique (Otte *et al.* 1900, Brincker *et al.* 2000). Then, the identified modal properties are used as features to estimate damages. Element-level damage assessments of bridge structures are performed using the neural networks technique.

A multi-stage diagnosis strategy aims at successive detection of the occurrence, location and extent of the structural damage (Ko *et al.* 2002, Qu *et al.* 2003). It has many advantages such as efficiency in computational time and better estimation accuracy. Moreover, it is suitable for on-line monitoring scheme. In a multi-stage approach, the assessment of damage severities is performed on the potentially damaged members, which have been identified in the previous stage. Accordingly, the damage assessment is undertaken on the less number of members, which can make the estimate results more accurate. In this study, two-step identification approaches are incorporated; the first step is for screening the potentially damaged members, and the second step is for detailed assessment of damage locations and severities. In the first step, three different methods were utilized: (1) Damage Indicator Method based on the Modal Strain Energy (DIM-MSE), (2) Probabilistic Neural Networks (PNNs), and (3) Neural Networks using Grouping technique (NNs-Gr). Then, in the second step the conventional neural networks (NNs) were utilized to assess the damage locations and severities on the screened members. Fig. 1 shows the flowchart for effective bridge health monitoring utilized in this study. The strain mode shapes calculated from the mode shapes are used as the input to DIM-MSE, and the mode shape differences between before and after damage, which are found to be less-sensitive to the modeling errors (Lee *et al.* 2005), are used as the input to PNNs and NNs to reduce the effect of modeling errors, since training patterns are to be generated from inaccurate FE model with modeling errors with considerable size. Theoretical backgrounds for damage detection methods utilized in this study are briefly explained.

Fig. 2 A plate with N_x by N_y sub-regions

2.1 Damage indicator method based on modal strain energy (DIM-MSE)

The damage indicator method based on modal strain energy (DIM-MSE), which constructs indices from various modal parameters, has been extensively adopted as one of the most effective methods for damage localization (Wang *et al.* 2000). Strain (or curvature) mode shape is sensitive to damage, because of its local behavior, and it has been utilized to locate damage sites in beams or frame structures (Pandey *et al.* 1991, Yao *et al.* 1992, Abdel Wahab and De Roeck 1999). When strain mode shape is used to identify damage in complex structural systems, such as plate-like structures, issues such as the establishment of an intuitive and effective damage sensitive index and the achievement of an accurate strain mode shape will be of great interest. Cornwell *et al.* (1999) extended the damage indicator method based on modal strain energy for beam-like structures to include the detection of damage in plate-like structures that are characterized by a two-dimensional curvature. Li *et al.* (2002) presented two novel damage sensitive parameters to determine the damage locations for plate-like structures, based on the continuity condition and the residual strain mode shape technique. In this study, a damage indicator method based on modal strain energy for plate-like structures is incorporated to detect damage locations of a bridge.

The damage index for the sub-region jk in Fig. 2 can be written as

$$\beta_{jk} = \frac{\sum_{i=1}^m f_{ijk}^*}{\sum_{i=1}^m f_{ijk}} \quad (2)$$

where

$$f_{ijk} = \frac{\int_{b_k}^{b_{k+1}} \int_{a_j}^{a_{j+1}} \left(\frac{\partial^2 \phi_i}{\partial x^2} \right)^2 + \left(\frac{\partial^2 \phi_i}{\partial y^2} \right)^2 + 2\nu \left(\frac{\partial^2 \phi_i}{\partial x^2} \right) \left(\frac{\partial^2 \phi_i}{\partial y^2} \right) + 2(1-\nu) \left(\frac{\partial^2 \phi_i}{\partial x \partial y} \right)^2 dx dy}{\int_0^b \int_0^a \left(\frac{\partial^2 \phi_i}{\partial x^2} \right)^2 + \left(\frac{\partial^2 \phi_i}{\partial y^2} \right)^2 + 2\nu \left(\frac{\partial^2 \phi_i}{\partial x^2} \right) \left(\frac{\partial^2 \phi_i}{\partial y^2} \right) + 2(1-\nu) \left(\frac{\partial^2 \phi_i}{\partial x \partial y} \right)^2 dx dy} \quad (3)$$

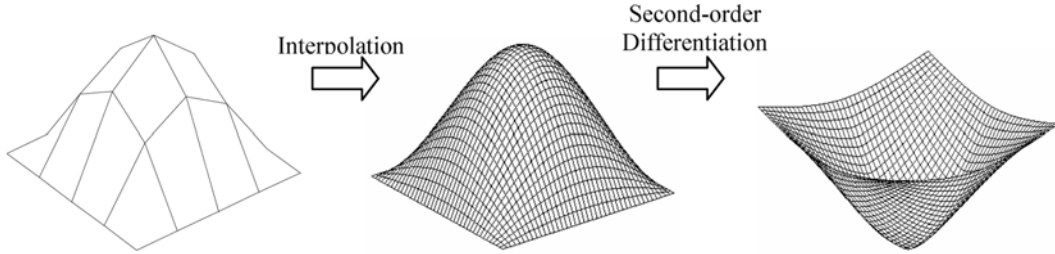


Fig. 3 Mode shape curvature from mode shape data

and m is the number of modes to be utilized. $\phi_i(x, y)$ is the i th mode shape of the undamaged state and ν is the Poisson ratio. The definitions of a , b , a_j and b_k are indicated in Fig. 2. An analogous term f_{ijk}^* can be defined using the damaged mode shape, $\phi_i^*(x, y)$. The above equation was derived by comparing the fractional strain energies at location jk of a plate before and after damage. More detailed derivations are explained in Cornwell *et al.* (1999).

In this study, mode shape curvatures (or strain mode shapes) were computed by numerically differentiating the identified mode shape vectors. At first, the mode shapes are identified from the acceleration data, and then the coarse mode shapes are interpolated into the finer ones using a cubic polynomial function. This is done because the number of sensors used for the mode shapes is limited, and the damage indicator method based on modal strain energy for plate-like structures requires many data points for better resolution. Fig. 3 illustrates the procedure used to calculate the finer mode shape curvatures from the coarse mode shape data. The effect of measurement noise on the mode shapes can be amplified in the mode shape curvatures, since they are calculated by second-order differentiation. To overcome the noise-sensitive characteristics of the mode shape curvatures, it is recommended to use sufficient records of measurement data, since the effects of noise can be largely alleviated through averaging. To remove the noise amplification in differential operations, the mode shape curvatures can be directly obtained from the dynamic strain data. As the technologies on smart sensors, such as optical fiber sensors, are being rapidly developed, the use of dynamic strain data to accurately calculate the strain mode shapes for the damage detection of bridge structures is an increasingly promising approach, which is beyond of the scope of this study.

2.2 Probabilistic neural networks (PNNs)

Probabilistic neural networks (PNNs) technique is basically a pattern classifier that combines the well-known Bayes decision strategy with the Parzen non-parametric estimator of the probability density functions of different classes (Specht 1990). PNNs have an advantage of quick calculation, since they are basically forward process. They do not need the training process as in the conventional neural networks. PNNs use supervised learning algorithms, and the training patterns are to be generated from the FE model, since it is difficult to obtain the information on the damaged structure. Training process in PNNs is just to allocate some training samples to a certain class. The class to be identified can be defined according to the damage mechanism, the type and location of structural members, the individual structural members etc.

Consider the two-category situation in which the state of nature θ is known to be either θ_A or θ_B . If it is desired to decide whether $\theta = \theta_A$ or $\theta = \theta_B$ based on a set of measurements represented

by the p -dimensional vector $\mathbf{X}^T = [X_1 \dots X_j \dots X_p]$, the Bayes decision rule becomes

$$d(\mathbf{X}) = \theta_A \text{ if } h_A l_A f_A(\mathbf{X}) > h_B l_B f_B(\mathbf{X}) \quad (4a)$$

$$d(\mathbf{X}) = \theta_B \text{ if } h_A l_A f_A(\mathbf{X}) < h_B l_B f_B(\mathbf{X}) \quad (4b)$$

where $f_A(\mathbf{X})$ and $f_B(\mathbf{X})$ are the probability density functions (PDFs) for categories A and B, respectively; l_A is the loss function associated with the decision $d(\mathbf{X}) = \theta_B$ when $\theta = \theta_A$; l_B is the loss associated with the decision $d(\mathbf{X}) = \theta_A$ when $\theta = \theta_B$ (the losses associated with correct decisions are taken to be equal to zero); h_A is the priori probability of occurrence of patterns from category A; and $h_B = 1 - h_A$ is the priori probability that $\theta = \theta_B$. In the simplified case that assumes both loss function and a priori probability are equal to each other, the Bayes rule classifies an input pattern to the class that has its PDF greater than the PDF of the other class. Therefore, the accuracy of the decision boundaries depends on the accuracy with which the underlying PDFs are estimated. Parzen (1962) showed how one may construct a family of estimates of $f(\mathbf{X})$, and Cacoullos (1966) has also extended Parzen's results to estimates in the special case that the multivariate kernel is a product of univariate kernels. In the particular case of the Gaussian kernel, the multivariate estimates can be expressed as

$$f_A(\mathbf{X}) = \frac{1}{(2\pi)^{p/2} \sigma^p m} \sum_{i=1}^m \exp \left[-\frac{(\mathbf{X} - \mathbf{X}_{Ai})^T (\mathbf{X} - \mathbf{X}_{Ai})}{2\sigma^2} \right] \quad (5)$$

where \mathbf{X} is the test vector to be classified; $f_A(\mathbf{X})$ is the value of the PDF of category A at point \mathbf{X} ; m is the number of training vectors in category A; p is the dimensionality of the training vectors; \mathbf{X}_{Ai} is the i th training vector for category A; and σ is the smoothing parameter. Note that $f_A(\mathbf{X})$ is simply the sum of small multivariate Gaussian distributions centered at each training sample. However, the sum is not limited to being Gaussian.

Probabilistic neural networks (PNNs) have been used for damage detection of bridge structures. Ni *et al.* (2000) applied PNNs to identify the damage type and location in the cable-stayed Ting Kau Bridge from the simulated noisy modal data. Cho *et al.* (2004) presented a two-step approach using PNNs to identify the damage location and the severity of damage using simulation data. Aoki *et al.* (2002) identified collapse mechanism of chemical plants using PNNs for seismic vulnerability assessment. The application of PNNs to damage detection of real structures is rare, since most of researches have been based on the simulation study.

In this study, PNNs are utilized to identify damage location based on the modal quantities. The class is defined according to the locations of structural members. Each class represents one of damage locations and the modal quantities of the damaged structure are training patterns belonging to that class. To reduce the number of classes to be identified, some neighboring elements are grouped to the same class. Training patterns representing a certain class are randomly generated by perturbing some element(s) in that class. The identified modal parameters are used as the input to PNNs. In this study, the mode shape differences between before and after damage, which are found to be less-sensitive to the modeling errors (Lee *et al.* 2005), were used as the input to the PNNs. Then PNNs calculate the probability of damage for each class, which indicates the similarity of the input to the training patterns in that class.

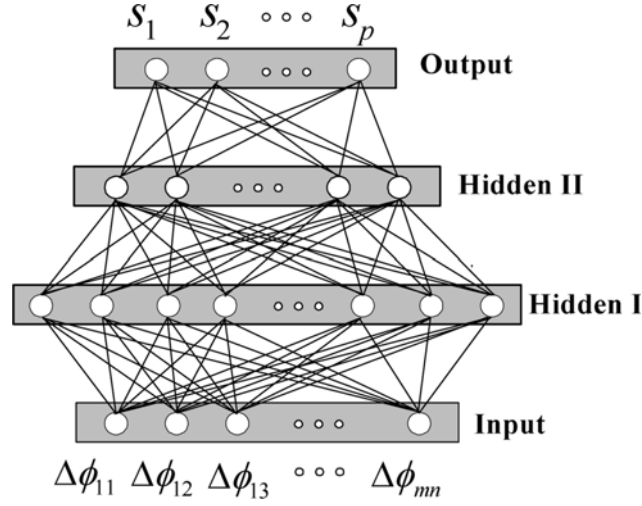


Fig. 4 Architecture of back-propagation neural networks

2.3 Neural networks by grouping technique (NNs-Gr)

In recent years, there has been increasing interest in the use of neural networks to estimate and predict the extent and location of damage in complex structures. In this study, a popular neural networks model called multi-layer perceptions with back-propagation algorithm was used to identify the element-level stiffness parameters (Matsuoka 1992, Yun and Bahng 2000, Yun *et al.* 2001, Lee *et al.* 2002). The networks consist of an input layer, two hidden layers, and an output layer, as shown in Fig. 4. In general, the neural networks with two hidden layers can build a complex decision boundary, whereas those with one hidden layer are appropriate for a simple problem and easy to implement. Sigmoid functions are utilized as nonlinear activation functions for all layers. The input layer contains the measured mode shape properties (i.e., the mode shape differences between before and after damage) and the output layer consists of the element-level stiffness indices to be identified as

$$S_i = k_i^d / k_i^0 \quad (6)$$

where k is element stiffness. Subscript i denotes the element number and subscripts 0 and d represent intact and damaged states, respectively. In this study, the element-level damage severity is defined as

$$\alpha_i = 1 - S_i \quad (7)$$

The input/output relationship of the neural networks can be nonlinear, as well as linear, and its characteristics are determined by the synaptic weights assigned to the connections between the neurons in two adjacent layers. A systematic way of updating the weights to achieve a desired input/output relationship based on a set of training patterns is referred to as a training or learning algorithm. In this study, the conventional back-propagation algorithm is adopted. Noise injection

learning (NIL) was also employed, to reduce the effect of measurement noise (Matsuoka 1992). In the NIL algorithm, the training is carried out using the artificially contaminated training patterns with noise of a prescribed level. The generalization capability of the neural networks under noisy conditions can be remarkably enhanced through this algorithm. Noise can be added to the training patterns as

$$\tilde{\mathbf{x}} = \mathbf{x} + \mathbf{v}_{N(0, \sigma)} \quad (8)$$

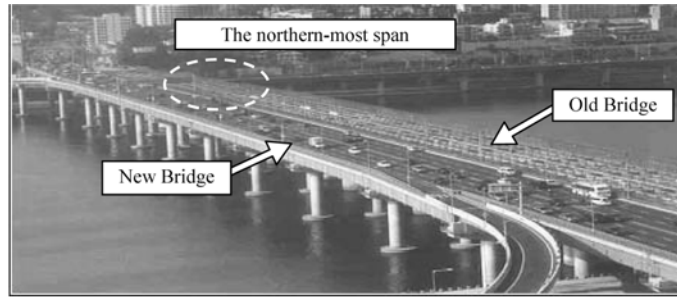
where $\tilde{\mathbf{x}}$ is a noise-injected input vector and \mathbf{x} is an exact input vector. The term $\mathbf{v}_{N(0, \sigma)}$ refers to Gaussian random noise with zero mean and standard deviation σ . The noise level σ is application specific. The noise described in the above equation indicates that signal-to-noise (S/N) ratios for all sensor locations are not equal, since the sensors mounted on different locations naturally suffer different uncertainties, even though the imposed noise level is nearly equal. Accordingly, a sensor with a low-amplitude signal will be exposed to a relatively high level of noise. There is no unique criterion to characterize the measurement noise, since the noise characteristics are application-specific. However, the noise level to be used in NIL can be properly assumed by examining the scattering characteristics of the measured data. For example, the noise level in the identified mode shapes, which were calculated from the acceleration time history of 60 minutes in length, can be pre-determined by examining the scattering characteristics of the mode shapes identified from lots of 30-minute acceleration data.

When the neural networks technique is used for damage detection of a bridge structure which is composed of a huge number of structural members, ill-posedness in the inverse problem is inevitable. To mitigate this problem, the grouping scheme can be effectively used. Elements with similar structural behavior or neighboring members can be included into one group. Using the grouping technique, the number of unknown parameters can be decreased. Accordingly, the complexity of the networks is also reduced. As in the PNNs, the mode shape differences between before and after damage are used as the input to the NNs, since training patterns are to be generated from inaccurate FE model with modeling errors with considerable size.

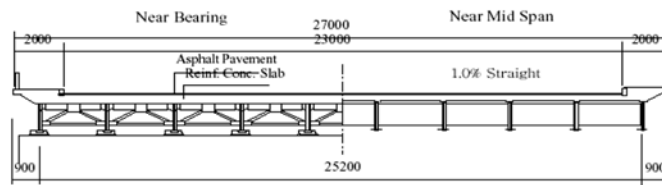
2.4 Second step for damage assessment using neural networks

In view of continuous monitoring of bridges, the damage assessment is not always needed to be carried out whereas the alarming for damages is to be continuously monitored. Therefore, the first step for screening the potentially damaged members needs quick calculation. More accurate damage estimation including the identification of damage locations and severities is to be performed, only when damage has occurred. Therefore, the second step can be carried out based on the results of the first step.

In this study, the conventional neural networks with back propagation algorithm are used for damage assessment in the second step. Only the potentially damaged members identified in the first step need to be considered in this networks configuration. In addition, only a few modal components measured in the potentially damaged regions are necessary to assess the damage locations and severities more accurately.



(a) Overview of old and new bridges



(b) Section view of old bridge

| | | | | | | | | | | | |
|-----|----|----|----|----|----|----|----|----|----|----|----|
| | 1 | 2 | 3 | 4 | 5 | 6 | 7 | 8 | 9 | 10 | 11 |
| G1 | | | R1 | | | | | | | | |
| G2 | 12 | 13 | 14 | 15 | 16 | 17 | 18 | 19 | 20 | 21 | 22 |
| G3 | | | R2 | | | | | | | | |
| G4 | 23 | 24 | 25 | 26 | 27 | 28 | 29 | 30 | 31 | 32 | 33 |
| G5 | | | R3 | | | | | | | | |
| G6 | 34 | 35 | 36 | 37 | 38 | 39 | 40 | 41 | 42 | 43 | 44 |
| G7 | | | R4 | | | | | | | | |
| G8 | 45 | 46 | 47 | 48 | 49 | 50 | 51 | 52 | 53 | 54 | 55 |
| G9 | | | R5 | | | | | | | | |
| G10 | 56 | 57 | 58 | 59 | 60 | 61 | 62 | 63 | 64 | 65 | 66 |
| G11 | | | R6 | | | | | | | | |
| G12 | 67 | 68 | 69 | 70 | 71 | 72 | 73 | 74 | 75 | 76 | 77 |
| G13 | | | R7 | | | | | | | | |
| G14 | | | | | | | | | | | |
| G15 | | | | | | | | | | | |

(c) Measurement locations (1-77: Roving sensor, R1-R7: Reference)

Fig. 5 Field test on the Hannam Grand Bridge in Seoul, Korea

3. Filed tests on the Hannam Grand Bridge

3.1 Description on the field tests

Field tests of damage estimation were performed on the northernmost span of the old Hannam Grand Bridge over the Han River in Seoul, Korea (Fig. 5), which is to be replaced during bridge renovation. The span is simply supported, with a length of 22.7 m. It is composed of nine steel plate girders and a concrete slab. Originally, it had ten girders, but the 10th girder was removed

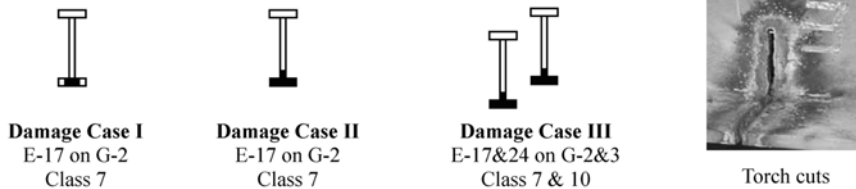
during the construction of the newly built bridge next to it.

Ambient vibration tests were carried out for the vertical accelerations on the bridge deck. The vibration was mainly induced by the traffic loads on the adjacent new bridge and by the train and vehicle loads under the test bridge. Seven sets of measurements were carried out on Girders 1 to 7, as shown in Fig. 5(c). For each set of measurements, vertical accelerations were measured at 11 equally spaced points on the slab just above each girder. Reference signals to correlate each experimental set were obtained at 7 points (R1-R7).

Fig. 6 shows the inflicted damage scenarios imposed by torch cuts on the main girders of the bridge for the present damage detection study. Modal parameters for each damage state were identified using the frequency domain decomposition method (Otte *et al.* 1900, Brincker *et al.* 2000). Table 1 shows the modal properties calculated from the initial finite element (FE) model and those estimated from the experiments for each damage case. The measured first natural frequencies do not show a close correlation to the imposed damages. This indicates the difficulty in using resonant frequencies as damage indicators for large civil engineering structures, where the environmental and operational effects such as temperature, humidity and traffic volume may not be ignored (Ko and Ni 2005). Accordingly, the natural frequency information was not used in the damage detection procedure. While the measured mode shapes are less sensitive to the

| | 1 | 2 | 3 | 4 | 5 | 6 | 7 | 8 | 9 | 10 | |
|-----------|----------|----|----------|----|----|----------|----|----|----------|----|--------------|
| G1 | Class 1 | | Class 2 | | | Class 3 | | | Class 4 | | |
| G2 | 11 | 12 | 13 | 14 | 15 | 16 | 17 | 18 | 19 | 20 | Damage I, II |
| | Class 5 | | Class 6 | | | Class 7 | | | Class 8 | | |
| G3 | 21 | 22 | 23 | 24 | 25 | 26 | 27 | 28 | 29 | 30 | Damage III |
| | Class 9 | | Class 10 | | | Class 11 | | | Class 12 | | |
| G4 | 31 | 32 | 33 | 34 | 35 | 36 | 37 | 38 | 39 | 40 | |
| | Class 13 | | Class 14 | | | Class 15 | | | Class 16 | | |
| G5 | 41 | 42 | 43 | 44 | 45 | 46 | 47 | 48 | 49 | 50 | |
| | Class 17 | | Class 18 | | | Class 19 | | | Class 20 | | |
| G6 | 51 | 52 | 53 | 54 | 55 | 56 | 57 | 58 | 59 | 60 | |
| | Class 21 | | Class 22 | | | Class 23 | | | Class 24 | | |
| G7 | 61 | 62 | 63 | 64 | 65 | 66 | 67 | 68 | 69 | 70 | |
| | Class 25 | | Class 26 | | | Class 27 | | | Class 28 | | |
| G8 | | | | | | | | | | | |
| G9 | | | | | | | | | | | |

(a) Damage locations and element/class numbers

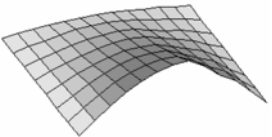
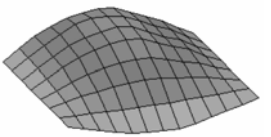
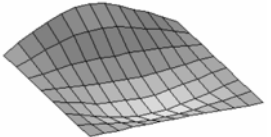


(b) Inflicted damages

Fig. 6 Damage scenarios for the Hannam Grand Bridge

Table 1 Natural frequencies and modes of the Hannam Grand Bridge

| Modes | | 1st mode | 2nd mode | 3rd mode |
|---------------------|------------|------------------|------------------|------------------|
| Calculated (Intact) | | 4.071 Hz | 4.452 Hz | 5.626 Hz |
| Measured | Intact | 4.247 Hz (99.79) | 4.876 Hz (97.86) | 5.771 Hz (99.71) |
| | Damage I | 4.188 Hz (99.38) | 4.903 Hz (99.45) | 5.823 Hz (99.64) |
| | Damage II | 4.196 Hz (99.90) | 4.780 Hz (99.35) | 5.778 Hz (99.57) |
| | Damage III | 4.218 Hz (99.51) | 4.757 Hz (99.56) | 5.799 Hz (99.73) |

| | | | |
|--|---|--|---|
| Measured mode shapes (Intact case) |  |  |  |
|--|---|--|---|

Note: Values in parentheses are the MAC values (%)

environmental effects, they may be significantly polluted by measurement errors (Ni *et al.* 2005). To alleviate the non-stationary characteristics of the ambient vibration tests and to reduce the measurement noise in the estimated mode shapes, it is strongly recommended to use sufficient records of measurement data, since the effects of noise can be largely alleviated through averaging. Noise injection learning algorithm in the neural networks is also employed to reduce the effect of measurement noise. In Table 1, the modal assurance criteria (MAC) values are also shown, which represent the closeness between the calculated and the experimental mode shapes. The first three modes gave close results to the test results: above 97% in MAC value. Therefore, the first three mode shapes were used as inputs for the damage estimation. The mode shapes were used to calculate the strain mode shape (the second derivative of mode shape) for the screening process, and the mode shape differences between before and after damage, which are found to be less-sensitive to the modeling errors, were used as the input to the neural networks (Lee *et al.* 2005).

3.2 Two-step approach I : DIM-MSE + NNs

In the first step, a damage indicator method based on modal strain energy (DIM-MSE) for plate-like structures was used to screen potentially damaged members of the test bridge. The first three modes for all of the intact and damaged cases, which are measured at 77 points with dimensions of 7 (girders) by 11 (sensor locations), were interpolated into the finer mode shapes using a cubic polynomial function, to numerically calculate the mode shape curvatures. Fig. 7 shows the damage indices calculated from DIM-MSE, along with the actually damaged locations. The bright locations correspond to the potentially damaged regions. The actually damaged location(s) was(were) identified with good accuracy for all damage cases, while there were some false damage alarms at several locations.

The basic scheme of DIM-MSE is to compare the strain mode shapes between before and after damage. Therefore, DIM-MSE requires a reference by which to estimate the current status. To examine the performance of DIM-MSE in view of continuous monitoring, damage locations are sequentially identified. Fig. 7(b) shows the sequentially estimated results obtained using DIM-MSE. The results of Damage Case I are equivalent to the results in Fig. 7(a). The damage indices for Damage Case II were calculated from the mode shapes of Damage Case I and Case II and the damage

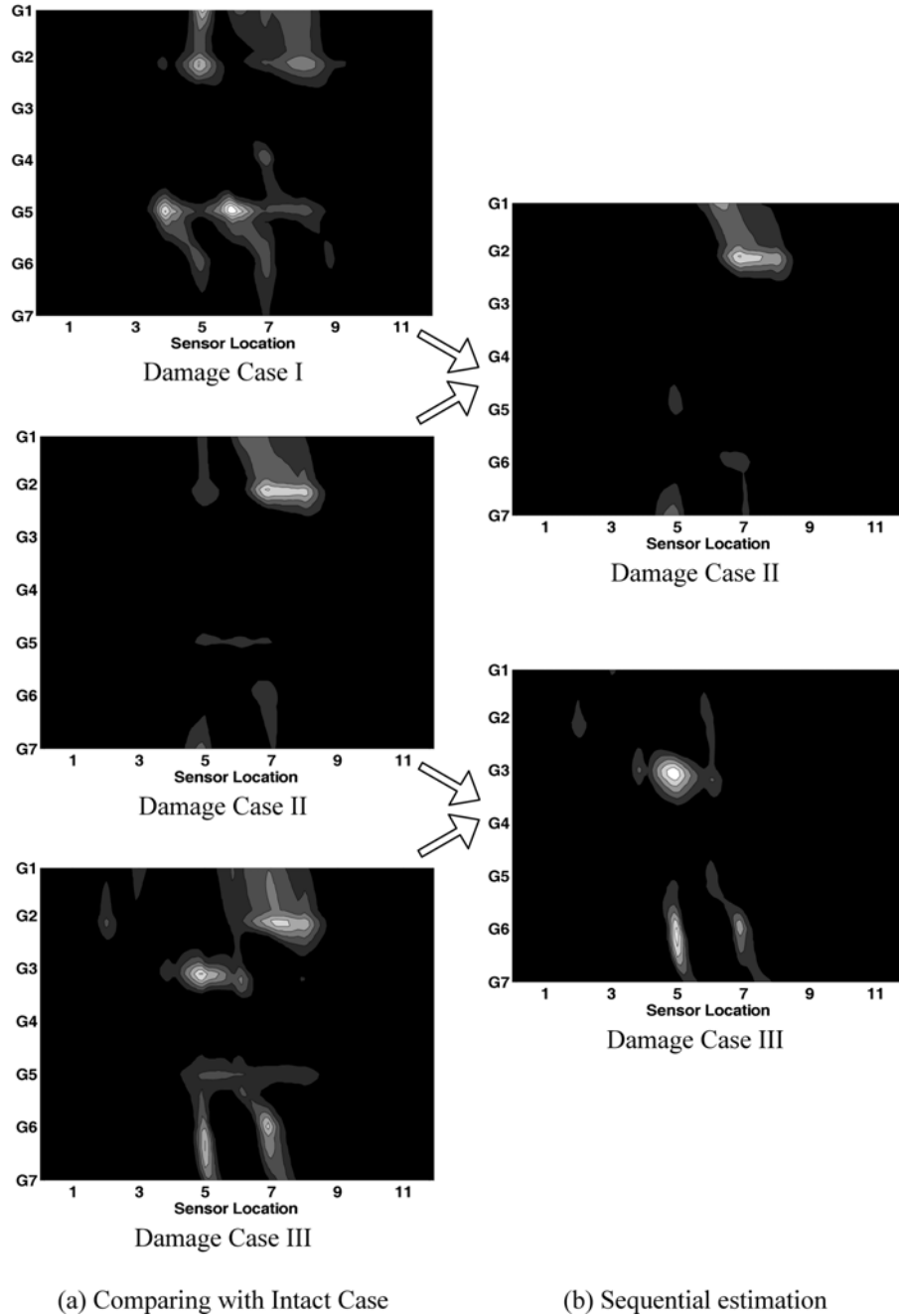
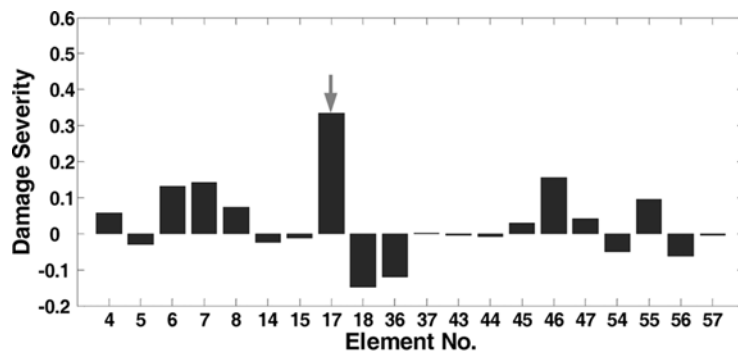


Fig. 7 Results of screening using DIM-MSE

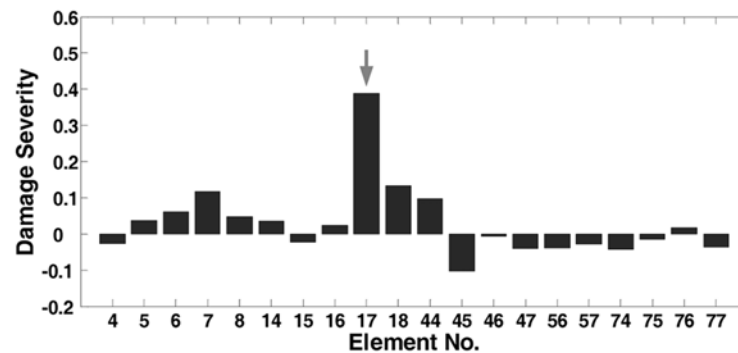
indices for Damage Case III were calculated from the mode shapes of Damage Case II and Case III. The additionally imposed damage was clearly identified from the sequential estimation results.

The conventional back-propagation neural networks technique with a noise injection learning algorithm was used for a detailed damage assessment. Only the potentially damaged members

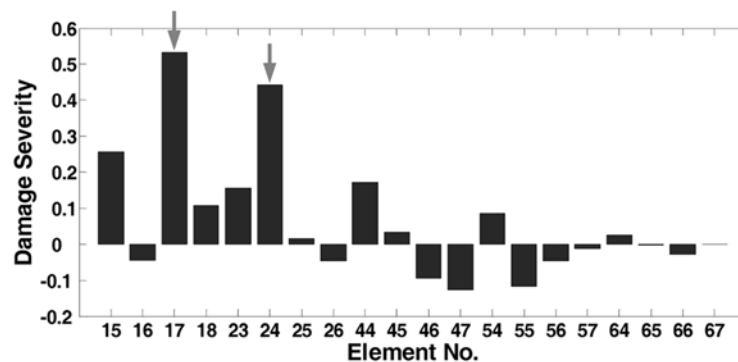
identified in the first step were considered in the networks configuration. The number of potentially damaged members to be investigated at the second step is user-defined, but it should be determined by considering the tradeoff between the network complexity and damage missing errors. The larger the number of potentially damaged members we choose is, the lower the damage missing errors is but the more complex the network configuration is. In this study, 20 elements with the higher damage indices out of 70 elements were selected as the potentially damaged members. The potentially damaged members considered in the second step were as follows:



(a) Damage Case I



(b) Damage Case II



(c) Damage Case III

Fig. 8 Results of damage assessment using NNs (↓: damaged locations)

Damage Case I: 20 Elements

Element 4, 5, 6, 7, 9, 14, 15, 17, 18, 36, 37, 43, 44, 45, 46, 47, 54, 55, 56, 57

Damage Case II: 20 Elements

Element 4, 5, 6, 7, 8, 14, 15, 16, 17, 18, 44, 45, 46, 47, 56, 57, 74, 75, 76, 77

Damage Case III: 20 Elements

Element 15, 16, 17, 18, 23, 24, 25, 26, 44, 45, 46, 47, 54, 55, 56, 57, 64, 65, 66, 67

Fig. 8 shows the results of the damage assessment using neural networks. The numbers of input, 1st hidden, 2nd hidden, and output nodes in the networks are 60-80, 20, 20 and 20, respectively. The number of input nodes is determined by considering the spatial distribution of the identified potentially damaged members and the magnitude of the mode shapes at those points. The mode shape data near the nodal points are excluded. The results of the damage assessment showed a good estimate for all the damage cases, even though there were many false alarms in the first step. The actually damaged member(s) showed large value(s) of damage severity and the members with false alarms showed small values, since the noise injection learning algorithm was effectively used to reduce the effect of noise.

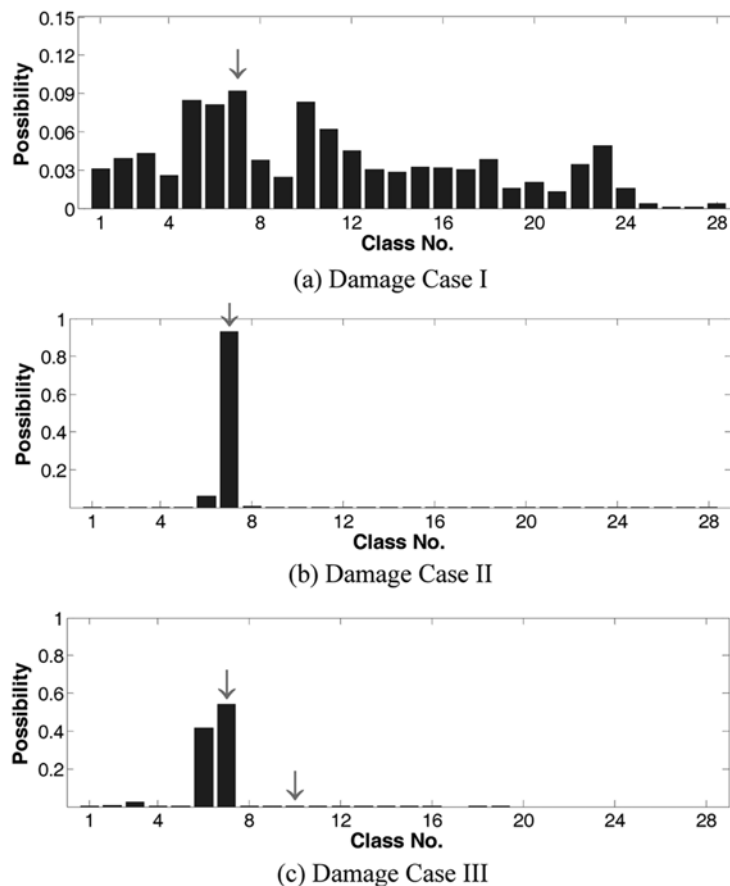


Fig. 9 Results of damage localization using PNNs

3.3 Two-step approach II : PNNs + NNs

Probabilistic neural networks technique was utilized in the first step for screening process. For the generation of training patterns, 28 classes were considered as shown in Fig. 6(a). Each class includes 2 or 3 elements. Training patterns for a certain class consists of 100 randomly generated damage cases. For each damage case, one element among 2 or 3 elements in the class is assumed damaged with 10 to 50% damage extent. For example, if Element 18 is assumed to be damaged, the class number corresponding to such damage scenario is 7. The class with the actually damaged member is Class 7 in Damage Case I and II, and Class 7 and 10 in Damage Case III. The mode shape differences between before and after damage were used as the input to PNNs and NNs.

Fig. 9 shows the results for screening potentially damaged members using the PNNs. The class with the actually damaged member is successfully identified for the cases with single damage (Damage Case I, II), whereas the screening process failed in Damage Case III with multiple damages. This is because the training patterns were generated for cases with single damage. There are several remedies to detect multiple damages using PNNs such as generating new classes, the conventional neural networks, and sequential prediction. New classes representing multiple damages can be generated. However, the number of combinations to cover the whole potential damage cases is too big to be utilized in the PNNs. For example, the number of combinations with 2 damage classes comes to ${}_{28}C_2$ (=378), and 3 damage classes to ${}_{28}C_3$ (=3276). The conventional neural networks technique can be an effective alternative to deal with the multiple damage cases. This approach is presented as the third two-step approach. If it is reasonable to assume that damage occurs sequentially not simultaneously, it is recommended that PNNs be applied to detect damage in sequence. Sequential prediction for multiple damage detection is applied to the field test on the Hannam Grand Bridge. Fig. 10 shows the results for screening process using sequential identification scheme. The additive damage on Girder 2 in Damage Case II and on Girder 3 in Damage Case III was successfully identified, although there was a false alarm at Class 14 in Damage Case III. From these results, it can be concluded that PNNs using sequential estimation scheme can be effectively used to detect multiple damage locations when the damage occurs sequentially not simultaneously.

Fig. 11 shows the result of damage assessment for Damage Case I, which showed lots of potentially damaged classes in the first step. The potentially damaged members corresponding to the classes identified in the first step were as follows:

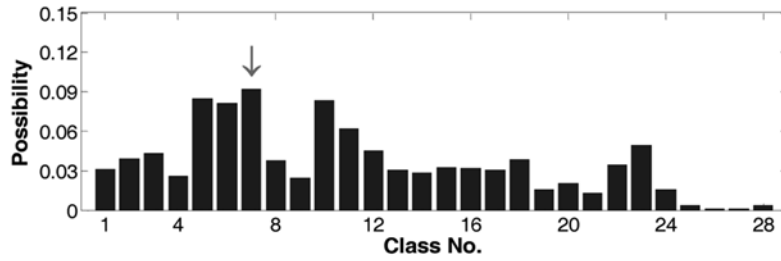
Class 5: Element 11, 12

Class 6: Element 13, 14, 15

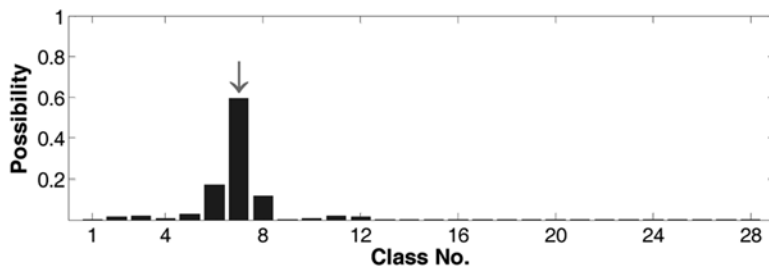
Class 7: Element 16, 17, 18

Class 10: Element 23, 24, 25

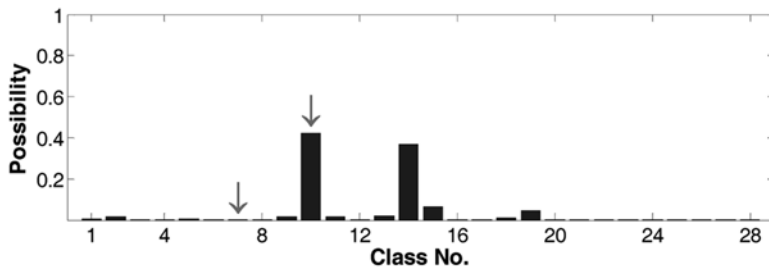
Totally 11 members were considered in the second step. Even though there were lots of false alarms in the first step, the results of damage assessment showed good estimate owing to the noise injection learning algorithm in NNs.



(a) Damage Case I



(b) Damage Case II



(c) Damage Case III

Fig. 10 Results of damage localization using PNNs: sequential estimation

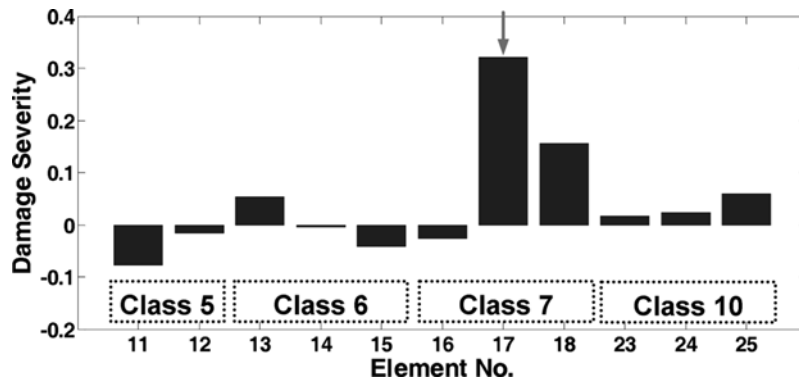


Fig. 11 Damage assessment for Damage Case I

3.4 Two-step approach III : NNs-Gr + NNs

To reduce the number of unknown parameter which is related to the networks complexity, the neural networks using grouping scheme (NNs-Gr) were used in the first step for screening. Twenty-eight groups similar to the classes in Fig. 6(a) were considered. For the generation of training patterns, several groups (up to five groups) were randomly selected and one element among 2 or 3 elements in those groups was assumed to be damaged with 10 to 50% damage extent. The required

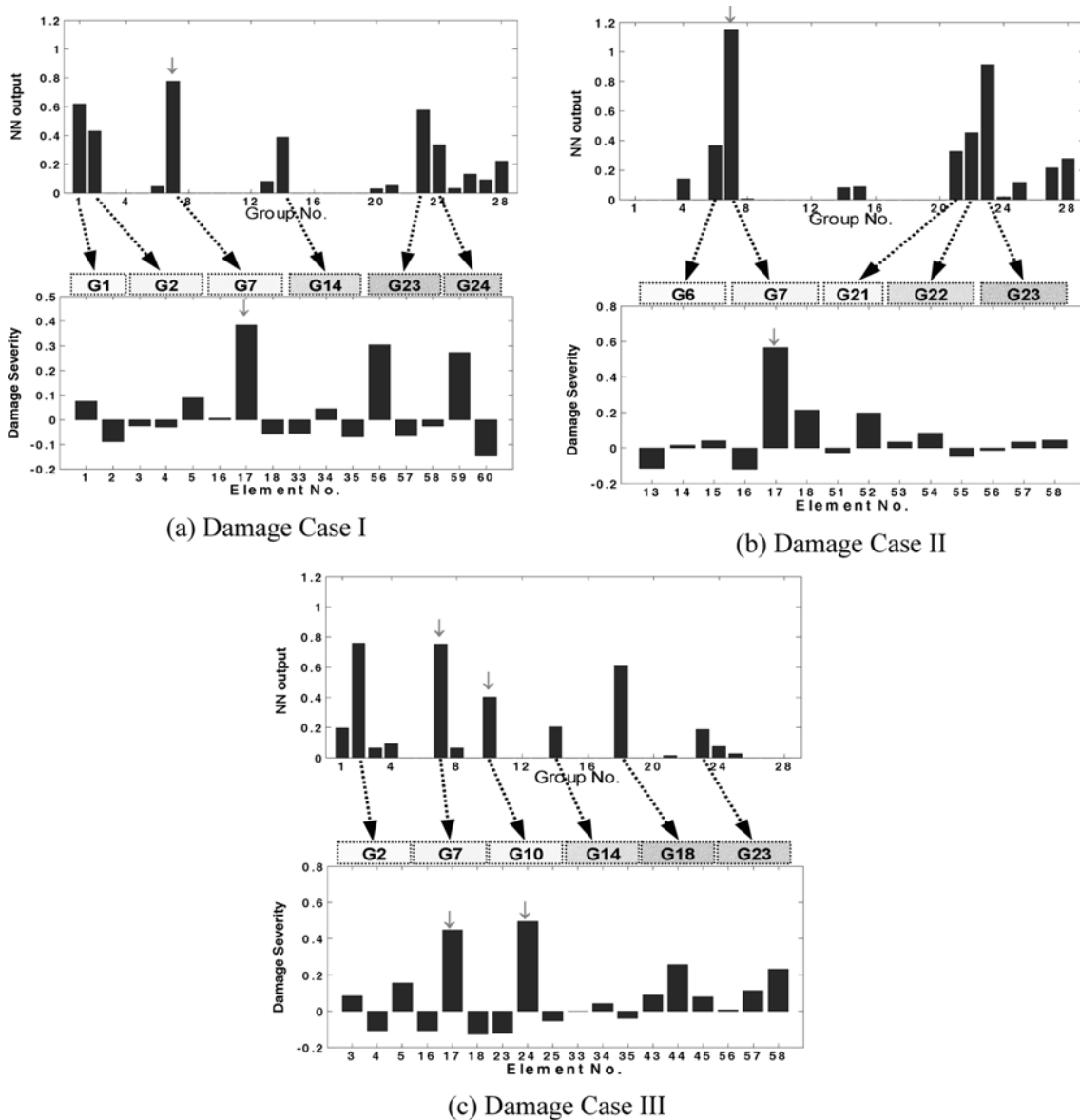


Fig. 12 Results of damage detection using NNs-Gr + NNs

output for intact case is null vector with the size of 28 which is the same number of total groups. If an element in a certain group is assumed to be damaged, a value of 1 is allocated to the corresponding position in the output vector. For example, if Element 21 and Element 34 in Fig. 6(a) is assumed damaged, the required output should be $[0^{(1)} 0^{(2)} \dots 0^{(8)} 1^{(9)} 0^{(10)} \dots 0^{(13)} 1^{(14)} 0^{(15)} \dots 0^{(28)}]$. The number of input nodes in the networks configuration is set to 96 excluding the mode shape data near the nodal points, and the number of output node is 28 same as the number of the total groups. In the second step, the conventional NNs technique was used based on the identified results in the first step. The potentially damaged members considered in the second step were as follows:

Damage Case I: Group 1, 2, 7, 14, 23, 24 (16 elements)

Element 1, 2, 3, 4, 5, 16, 17, 18, 33, 34, 35, 56, 57, 58, 59, 60

Damage Case II: Group 6, 7, 21, 22, 23 (14 elements)

Element 13, 14, 15, 16, 17, 18, 51, 52, 53, 54, 55, 56, 57, 58

Damage Case III: Group 2, 7, 10, 14, 18, 23 (18 elements)

Elements 3, 4, 5, 16, 17, 18, 23, 24, 25, 33, 34, 35, 43, 44, 45, 56, 57, 58

Fig. 12 shows the results of damage localization using NNs-Gr and the results of damage assessment using NNs. The results of damage localization showed more false alarms than the results of using PNNs. This is because there are lots of local minima of the networks in the training process. The non-uniqueness of the solution due to the local minima during the parameter estimation, noise, and limited number of measurements may be resolved by employing the committee technique (Perrone and Cooper 1993), which is beyond the scope of this thesis. Nevertheless, Damage Case III with multiple damages was reasonably identified not missing the actually damaged members, when NNs-Gr was utilized in the first step. It has been found that all the damage locations were reasonably identified for all cases. However, the estimated results contain false alarms with fairly large magnitudes at several locations, especially in Damage Case I and Damage Case III.

Table 2 Comparison results for two-step approaches

| | DIM-MSE + NNs | PNNs + NNs | NNs-Gr + NNs |
|---------------------------|---|---|---|
| Advantage | <ul style="list-style-type: none"> ✓ sensitive to damage ✓ can detect multiple damages | <ul style="list-style-type: none"> ✓ can deal with noise ✓ can use various input ✓ good estimate for single damage | <ul style="list-style-type: none"> ✓ can deal with noise ✓ can use various input ✓ can detect multiple damages |
| Disadvantage | <ul style="list-style-type: none"> ✓ sensitive to noise ✓ accurate modes need to be evaluated | <ul style="list-style-type: none"> ✓ difficult to detect multiple damages | <ul style="list-style-type: none"> ✓ time consuming in training ✓ lots of local minima |
| Remedies for shortcomings | <ul style="list-style-type: none"> ✓ obtain strain mode shapes directly ✓ use average of many data sets | <ul style="list-style-type: none"> ✓ sequential estimation for multiple damages | <ul style="list-style-type: none"> ✓ parallel computing ✓ committee neural networks |

4. Conclusions

In this study, two-step identification strategies were proposed for effective monitoring of bridge structures to alleviate ill-posedness problem in the neural networks-based damage detection. Three different methods were utilized in the first step for screening: (1) Damage Indicator Method based on the Modal Strain Energy (DIM-MSE), (2) Probabilistic Neural Networks (PNNs), and (3) Neural Networks using Grouping technique (NNs-Gr). In the second step, the conventional neural networks technique was utilized to assess damage locations and damage severities. Two-step approaches were applied to the field test on the Hannam Grand Bridge to demonstrate the effectiveness of the present methods. Three different combinations of damage localization and damage assessment methods have unique characteristics depending on the first step methods utilized. The results can be summarized in Table 2.

A damage indicator method based on modal strain energy (DIM-MSE) has an advantage of being sensitive to damage, whereas it has a disadvantage of being sensitive to noise. To overcome the noise-sensitive feature, it is recommended to use sufficient records of measurement data, since the effects of noise can be largely alleviated through averaging and the measurement data sets can be easily accumulated in the monitoring system. To remove the noise amplification in differential operations, it is challenging to use the strain mode shapes directly obtained from the dynamic strain data.

The effect of measurement noise can be reduced by noise injection learning algorithm in PNNs and NNs, but it is difficult to obtain an accurate baseline model to be used for the generation of training patterns. This problem can be overcome by using the modal quantities less sensitive to the modeling errors, i.e., the mode shape differences between before and after damage. It has been found that the multiple damages were detected by using DIM-MSE or NNs-Gr, though PNNs gave accurate estimate for single damage locations. To detect multiple damages using PNNs, it has been suggested to use the sequential estimation scheme. The additive damage in Damage Case II and Damage Case III was successfully identified using the sequential estimation scheme. NNs-Gr can detect multiple damages but showed large errors.

In general, to make the bridge health monitoring system more applicable and reliable, it is recommended to use various damage detection methods available to avoid the damage missing errors at the first step. Note that DIM-MSE and PNNs are appropriate for large structures whereas NNs-Gr can be applied to moderate-size structures; DIM-MSE should be utilized when the measurement noise is small; and PNNs should be applied to the continuous monitoring system not to miss the multiple damages.

Acknowledgements

This study is supported by Smart Infra-Structure Technology Center (SISTeC) at KAIST, which is sponsored by Ministry of Science and Technology (MOST) and the Korea Science and Engineering Foundation (KOSEF). Their financial supports are greatly acknowledged.

References

- Abdel Wahab, M.M. and De Roeck, G. (1999), "Damage detection in bridges using modal curvatures: Application to a real damage scenario", *J. Sound Vib.*, **226**(2), 217-235.
- Aoki, T., Ceravolo, R., De Stefano, A., Genovese, C. and Sabia, D. (2002), "Seismic vulnerability assessment of chemical plants through probabilistic neural networks", *Reliability Engineering & System Safety*, **77**(3), 263-268.
- Brincker, R., Zhang, L. and Andersen, P. (2000), "Modal identification from ambient response using frequency domain decomposition", *Proc. of 18th Int. Modal Analysis Conf.*, 625-630, San Antonio, TX, USA.
- Cacoullos, T. (1966), "Estimation of a multivariate density", *Annals of the Institute of Statistical Mathematics*, **18**(2), 179-189, Tokyo, Japan.
- Cawley, P. and Adams, R.D. (1979), "Location of defects in structures from measurements of natural frequencies", *J. Strain Anal.*, **14**(2), 49-57.
- Chance, J., Tomlinson, G.R. and Worden, K. (1994), "Simplified approach to the numerical and experimental modeling of the dynamics of a cracked beam", *Proc., 12th Int. Modal Analysis Conf.*, Honolulu, **1**, 778-785.
- Cho, H.N., Choi, Y.M., Lee, S.C. and Hur, C.K. (2004), "Damage assessment of cable stayed bridge using probabilistic neural network", *Struct. Eng. Mech.*, **17**(3-4), 483-492.
- Cornwell, P., Doebling, S.W. and Farrar, C.R. (1999), "Application of the strain energy damage detection method to plate-like structures", *J. Sound Vib.*, **224**(2), 359-374.
- Crohas, H. and Lepert, P. (1982), "Damage detection monitoring method for offshore platforms is field tested", *Oil & Gas J.*, **80**(8), 94-103.
- Kim, J.T. and Stubb, N. (1995), "Model uncertainty impact and damage-detection accuracy in plate girder", *J. Struct. Eng.*, ASCE, **121**(10), 1409-1417.
- Ko, J.M., Sun, Z.G. and Ni, Y.Q. (2002), "Multi-stage identification scheme for detecting damage in cable-stayed Kap Shui Mun Bridge", *Eng. Struct.*, **24**, 857-868.
- Ko, J.M. and Ni, Y.Q. (2005), "Technology developments in structural health monitoring of large-scale bridges", *Eng. Struct.*, **27**(12), 1715-1725.
- Lee, J.W., Kim, J.D., Yun, C.B., Yi, J.H. and Shim, J.M. (2002), "Health-monitoring method for bridges under ordinary traffic loadings", *J. Sound Vib.*, **257**(2), 247-264.
- Lee, J.J., Lee, J.W., Yi, J.H., Yun, C.B. and Jung, H.Y. (2005), "Neural networks-based damage detection for bridges considering errors in baseline finite element models", *J. Sound Vib.*, **280**, 555-578.
- Li, Y.Y., Cheng, L., Yam, L.H. and Wong, W.O. (2002), "Identification of damage locations for plate-like structures using damage sensitive indices: strain modal approach", *Comput. Struct.*, **80**, 1881-1894.
- Matsuoka, K. (1992), "Noise injection into inputs in back-propagation learning", *IEEE Transaction of Systems, Man, and Cybernetics*, **22**(3), 436-440.
- Ni, Y.Q., Zhou, X.T., Ko, J.M. and Wang, B.S. (2000), "Vibration-based damage localization in Ting Kau Bridge using probabilistic neural network", *Advances in Structural Dynamics*, J.M. Ko and Y.L. Xu (eds.), Elsevier Science Ltd., Oxford, UK, Vol. **II**, 1069-1076.
- Ni, Y.Q., Fan, K.Q., Zheng, G., Ko, J.M. (2005), "Automatic modal identification and variability in measured vectors of a cable-stayed bridge", *Struct. Eng. Mech.*, **19**(2), 123-139.
- Otte, D., Van de Ponselee, P. and Leuridan, J. (1990), "Operational shapes estimation as a function of dynamic loads", *Proc. of the 8th Int. Modal Analysis Conf.*, 413-421.
- Pandey, A.K., Biswas, M. and Samman, M.M. (1991), "Damage detection from changes in curvature mode shape", *J. Sound Vib.*, **145**, 312-332.
- Parzen, E. (1962), "On estimation of a probability density function and mode", *Annals of Mathematical Statistics*, **33**, 1065-1076.
- Perrone, M.P. and Cooper, L.N. (1993), "When networks disagree: ensemble methods for hybrid neural networks", *Artificial Neural Networks for Speech and Vision*, Chapman & Hall, London, 126-142.
- Qu, W.L., Chen, W. and Xiao, Y.Q. (2003), "A two-step approach for joint damage diagnosis of framed structures using artificial neural networks", *Struct. Eng. Mech.*, **16**(5), 581-595.
- Rytter, A. (1993), "Vibration based inspection of civil engineering", Ph.D. Dissertation, University of Aalborg, Denmark.

- Specht, D.F. (1990), "Probabilistic neural networks", *Neural Networks*, **3**, 109-118.
- Stubbs, N., Park, S., Sikorsky, C. and Choi, S. (2000), "Global nondestructive damage assessment methodology for civil engineering structures", *Int. J. Syst. Sci.*, **31**(11), 1361-1373.
- Vandiver, J.K. (1975), "Detection of structural failures on fixed platforms by measurement of dynamic responses", *Proc., 7th Annual Offshore Technology Conf.*, Houston.
- Wang, M.L., Xu, F.L. and Lloyd, G.M. (2000), "Results and implications of the damage index method applied to a multi-span continuous segmental prestressed concrete bridge", *Struct. Eng. Mech.*, **10**(1), 37-51.
- Wu, X., Ghaboussi, J. and Garret, J.H., Jr. (1992), "Use of neural networks in detection of structural damage", *Comput. Struct.*, **42**(4), 649-659.
- Yao, G.C., Chang, K.C. and Lee, G.C. (1992), "Damage diagnosis of steel frames using vibrational signature analysis", *J. Eng. Mech.*, ASCE, **118**(9), 1949-1961.
- Yun, C.B. and Bahng, E.Y. (2000), "Substructural identification using neural networks", *Comput. Struct.*, **77**(1), 41-52.
- Yun, C.B., Yi, J.H. and Bahng, E.Y. (2001), "Joint damage assessment of framed structures using neural networks technique", *Eng. Struct.*, **23**(5), 425-435.